Conclusion

In this paper, the *in vitro* and *in vivo* antitumor activities and lymphatic migration of water-dispersed and anticancer-drug-bound oxSWNHs (PEG–DXR–oxSWNH) have been described. i.t. administration of PEG–DXR– oxSWNHs was effective in reducing tumor growth in tumor-bearing mice. The physical binding of PEG–DXR to the oxSWNH surface and the retention of oxSWNHs themselves in the NCI-H460 tumor contributed to the *in vivo* effectiveness in terms of prolonged exposure of DXR derivatives to the tumor. Unexpectedly, oxSWNHs were found to migrate specifically to the adjacent axillary lymph node after i.t. administration of PEG–DXR–oxSWNHs. This limited distribution of water-dispersed oxSWNHs around the injection site indicates clearly that they would be suitable drug carriers for local chemotherapy.

Future perspective

The effectiveness of the local route of administration of antitumor drugs, compared with the systemic route, has been gaining increasing attention, as described earlier. We observed that i.t. injected PEG–DXR–oxSWNHs migrated, in part, selectively to the adjacent axillary lymph node. The axillary lymph node is known to be an organ in which breast cancer metastasis often occurs [32,33]. A recent study suggested that local administration of PEGylated liposomal doxorubicin into the mammary ductal network of a mouse model of breast cancer prevented tumor development more effectively than systemic administration [23]. Taken together, water-dispersed oxSWNHs are expected to be novel drug carriers for local chemotherapy against solid tumors with lymph-node metastasis. The antitumor activity of the complexes should be augmented by linker refinement in PEG–DXR and/or small-drug deposition (e.g., cisplatin) in their interior space. Such refinement toward therapy for the mouse model of metastatic breast cancer is underway. At the same time, we are preparing smaller oxSWNHs, which are expected to be excreted more easily from the body. Smaller oxSWNHs would shed light on the systemic administration of water-dispersed oxSWNHs.

Acknowledgments

The authors thank Jing Fan for synthesis and TEM analysis of oxidized carbon nanohorns.

Financial & competing interests disclosure

This research was in part supported by a grant-in-aid for Young Scientists (B) (19790143) to T.M., a grant-in-aid for Exploratory Research (18659080) to K.T. and a grant-in-aid for the 21st Century Center of Excellence Program of Fujita Health University from the Ministry of Education, Culture, Sports, Science, and Technology of Japan. The authors have no other relevant affiliations or financial involvement with any organization or entity with a financial interest in or financial conflict with the subject matter or materials discussed in the manuscript apart from those disclosed.

No writing assistance was utilized in the production of this manuscript.

Executive summary

Oxidized single-wall carbon nanohorn

- Oxidized single-wall carbon nanohorns (OxSWNHs) can store drugs both in the tube interior space and on the outer surface. Multidrug therapy may be achievable with oxSWNHs concomitantly retaining two different drugs.

Water-dispersed oxSWNHs with antitumor activity

- PEG–DXR-bound oxSWNHs (PEG–DXR–oxSWNHs) showed lower *in vitro* antitumor activity, whereas they had slightly higher *in vivo* antitumor activity than free PEG–DXR.
- The tumor tissues of intratumorally PEG–DXR–oxSWNH-treated mice retained 61% of total injected DXR even 2 weeks after the first injection. Higher *in vivo* antitumor activity of PEG–DXR–oxSWNHs could be explained, at least in part, by this high DXR retention ability of oxSWNH in the tumor tissue.
- A part of oxSWNHs in the tumor tissues of mice migrated to and retained in the axillary lymph nodes, which are major sites of breast cancer metastasis. This observation suggests the possibility of water-dispersed oxSWNHs as drug carriers targeting lymph node metastasis in breast cancer.

Problems to be solved toward practical applications

- Potentiation of the antitumor activity of water-dispersed oxSWNHs; for example, by linker refinement in PEG–DXR and/or small drug storage in the tube interior space, is needed.

Ethical conduct of research

The authors state that they have obtained appropriate institutional review board approval or have followed the principles outlined in the Declaration of Helsinki for all human or animal experimental investigations. In addition, for investigations involving human subjects, informed consent has been obtained from the participants involved.

Bibliography

1. Muggia FM: Liposomal encapsulated anthracyclines: new therapeutic horizons. *Curr. Oncol. Rep.* 3, 156–162 (2001).
2. Mizushima Y, Hoshi K: Review: recent advances in lipid microsphere technology for targeting prostaglandin delivery. *J. Drug Target.* 1, 93–100 (1993).
3. Adler-Moore J, Proffitt RT: AmBisome: liposomal formulation, structure, mechanism of action and pre-clinical experience. *J. Antimicrob. Chemother.* 49(Suppl. 1), 21–30 (2002).
4. Okada H, Heya T, Ogawa Y, Toguchi H, Shimamoto T: Sustained pharmacological activities in rats following single and repeated administration of once-a-month injectable microspheres of leuprolide acetate. *Pharm. Res.* 8, 584–587 (1991).
5. Nishiyama N, Kataoka K: Current state, achievements and future prospects of polymeric micelles as nanocarriers for drug and gene delivery. *Pharmacol. Ther.* 112, 630–648 (2006).
6. Ren L, Chow GM: Synthesis of nir-sensitive Au–Au_2S nanocolloids for drug delivery. *Mater. Sci. Eng.* 23, 113–116 (2003).
7. Iijima S, Yudasaka M, Yamada R *et al.*: Nano-aggregates of single-walled graphitic carbon nano-horns. *Chem. Phys. Lett.* 309, 165–170 (1999).
8. Ajima K, Yudasaka M, Suenaga K, Kasuya D, Azami T, Iijima S: Material storage mechanism in porous nanocarbon. *Adv. Mater.* 16, 397–401 (2004).
9. Miyawaki J, Yudasaka M, Azami T, Kubo Y, Iijima S: Toxicity of single-walled carbon nanohorns. *ACS NANO* 2, 227–234 (2008).
10. Murakami T, Ajima K, Miyawaki J, Yudasaka M, Iijima S, Shiba K: Drug-loaded carbon nanohorns: adsorption and release of dexamethasone *in vitro*. *Mol. Pharm.* 1, 399–405 (2004).
11. Ajima K, Yudasaka M, Murakami T, Maigne A, Shiba K, Iijima S: Carbon nanohorns as anticancer drug carriers. *Mol. Pharm.* 2, 475–480 (2005).
12. Murakami T, Fan J, Yudasaka M, Iijima S, Shiba K: Solubilization of single-wall carbon nanohorns using a PEG–doxorubicin conjugate. *Mol. Pharm.* 3, 407–414 (2006).
13. Liu Z, Davis C, Cai W, He L, Chen X, Dai H: Circulation and long-term fate of functionalized, biocompatible single-walled carbon nanotubes in mice probed by Raman spectroscopy. *Proc. Natl Acad. Sci. USA* 105, 1410–1415 (2008).
14. Isobe H, Tanaka H, Maeda R *et al.*: Preparation, purification, characterization, and cytotoxicity assessment of water-soluble, transition-metal-free carbon nanotube aggregates. *Angew. Chem. Int. Ed.* 45, 6676–6680 (2006).
15. Cui D, Tian F, Ozkan CS, Wang M, Gao H: Effect of single wall carbon nanotubes on human HEK293 cells. *Toxicol. Lett.* 155, 73–85 (2005).
16. Wörle-Knirsch JM, Pulskamp K, Krug F: Oops they did again! Carbon nanotubes hoax scientists in viability assays. *Nano Lett.* 6, 1261–1268 (2006).
17. Cherukuri P, Gannon CJ, Leeuw TK *et al.*: Mammalian pharmacokinetics of carbon nanotubes using intrinsic near-infrared fluorescence. *Proc. Natl Acad. Sci. USA* 103, 18882–18886 (2006).
18. Lacerda L, Ali-Boucetta H, Herrero MA *et al.*: Tissue histology and physiology following intravenous administration of different types of functionalized multiwalled carbon nanotubes. *Nanomed.* 3, 149–161 (2008).
19. Armstrong DK, Bundy B, Wenzel L *et al.*: Intraperitoneal cisplatin and paclitaxel in ovarian cancer. *N. Engl. J. Med.*. 354, 34–43 (2006).
20. Hagiwara A, Takahashi T, Kojima O *et al.*: Prophylaxis with carbon-adsorbed mitomycin against peritoneal recurrence of gastric cancer. *Lancet* 339, 629–631 (1992).
21. Yan TD, Black D, Sugarbaker PH *et al.*: A systemic review and meta-analysis of the randomized controlled trials on adjuvant intraperitoneal chemotherapy for resectable gastric cancer. *Ann. Surg. Oncol.* 14, 2702–2713 (2007).
22. Ikehara Y, Niwa T, Biao L *et al.*: A carbohydrate recognition-based drug delivery and controlled release system using intraperitoneal macrophages as a cellular vehicle. *Cancer Res.* 66, 8740–8748 (2006).
23. Murata S, Kominsky SL, Vali M *et al.*: Ductal access for prevention and therapy of mammary tumors. *Cancer Res.* 66, 638–645 (2006).
24. Fan J, Yudasaka M, Kasuya D *et al.*: Micrometer-sized graphitic balls produced together with single-wall carbon nanohorns. *J. Phys. Chem. B* 109, 10756–10759 (2005).
25. Murata K, Kaneko K, Steele WA *et al.*: Molecular potential structures of heat-treated single-wall carbon nanohorn assemblies. *J. Phys. Chem. B* 105, 10210–10216 (2001).
26. Veronese FM, Schiavon O, Pasut G *et al.*: PEG–doxorubicin conjugates: influence of polymer structure on drug release, *in vitro* cytotoxicity, biodistribution, and antitumor activity. *Bioconjugate Chem.* 16, 775–784 (2005).
27. Negishi H, Takeda M, Fujimoto T *et al.*: Lymphatic mapping and sentine node identification as related to the primary sites of lymph node metastasis in early stage ovarian cancer. *Gynecol. Oncol.* 94, 161–166 (2004).
28. Hagiwara A, Takahashi T, Sawai K *et al.*: Lymph nodal vital staining with newer carbon particle suspenshions compared with India ink: experimental and clinical observations. *Lymphology* 25, 84–89 (1992).
29. Stevens A, Lowe J: *Human Histology (2nd Edition)*. Mosby, Times Mirror International Publishers Ltd, London, UK (1997).
30. Gorczyca W, Bigman K, Mittelman A *et al.*: Induction of DNA strand breaks associated with apoptosis during treatment of leukemias. *Leukemia* 7, 659–670 (1993).
31. Schmied GM, Giegerich G, Breitschopf H, Hartung HP, Toyka KV, Lassmann H: Differentiation between cellular apoptosis and necrosis by the combined use of *in situ* tailing and nick translation techniques. *Lab. Invest.* 71, 219–225 (1994).
32. Giuliano AE, Kirgan DM, Michael Guenther J, Morton DL: Lymphatic mapping and sentinel lymphadenectomy for breast cancer. *Ann. Surg.* 220, 391–401 (1994).
33. Krag D, Weaver D, Ashikaga T *et al.*: The sentinel node in breast cancer. *N. Engl. J. Med.* 339, 941–946 (1998).

Current Opinion in Drug Discovery & Development 2008 11(4):487-494
 ISSN 1367-6733

Targeting myostatin for therapies against muscle-wasting disorders

Kunihiro Tsuchida

Address
Division for Therapies against Intractable Diseases, Institute for Comprehensive Medical Science (ICMS), Fujita Health University, Toyoake, Aichi 470-1192, Japan
Email: tsuchida@fujita-hu.ac.jp

In addition to gene correction therapy and cell transplantation techniques, multidisciplinary approaches to drug discovery and development offer promising therapeutic strategies for intractable genetic muscular disorders including muscular dystrophy. Inhibition of the production and activity of myostatin, a potent growth factor that determines skeletal muscle size, is a novel strategy for the treatment of muscle-wasting disorders such as muscular dystrophy, cachexia and sarcopenia. Myostatin blockers include myostatin-blocking antibodies, myostatin propeptide, follistatin and follistatin-related proteins, soluble myostatin receptors, small interfering RNA and small chemical inhibitors. This review describes the discovery and development of myostatin inhibitors.

Keywords Myostatin, muscle-wasting disorders, muscular dystrophy, myostatin propeptide, activin receptors, follistatin

Abbreviations

ActR activin receptor, **ALK** activin receptor-like kinase, **BMP** bone morphogenetic protein, **DMD** Duchenne muscular dystrophy, **FLRG** follistatin-related gene, **GDF** growth and differentiation factor, **LGMD** limb-girdle muscular dystrophy, **RNAi** RNA interference, **TGF-β** transforming growth factor-β

Introduction

The transforming growth factor-β (TGF-β) superfamily is the largest growth factor subfamily and includes TGF-βs, activin, myostatin and bone morphogenetic proteins (BMPs) [1]. Among these growth factors, myostatin plays an essential role in the negative regulation of muscle growth and determines the mass and size of skeletal muscle [1-3]. The inhibition of myostatin activity is a promising therapeutic strategy for restoring muscle mass and strength in muscle-wasting disorders such as muscular dystrophy, cachexia and sarcopenia [1-4]. As with other growth factors in the TGF-β superfamily, the actions of myostatin are tightly regulated by multiple molecular mechanisms [2]. The production of myostatin is controlled by the processing of precursor proteins. In addition, extracellular binding proteins limit the actions of active myostatin. Signal transduction of myostatin occurs via cell surface transmembrane serine/threonine kinase receptors and intracellular Smad proteins [5,6]. Thus, the activity of myostatin is also tightly controlled within the cell. Potential myostatin inhibitors such as myostatin-blocking antibodies, myostatin propeptide, follistatin domain-containing proteins, soluble myostatin receptors, antisense and small interfering RNA, and chemical TGF-β-inhibiting compounds are being developed. These inhibitors and their derivatives could provide new drugs for the treatment of muscle-wasting disorders. This review describes the development of a clinically useful strategy for targeting myostatin.

Structure and activation of myostatin

Myostatin, also known as growth and differentiation factor-8 (GDF-8), was identified through screening of a novel member of the TGF-β superfamily (Figure 1) [7••]. Myostatin is almost exclusively expressed in skeletal muscle, but it is also found, to a lesser extent, in adipose tissues. Myostatin gene-deleted mice were demonstrated to have hypermuscular phenotypes [7••]. Both an increased number of muscle fibers and an increased fiber size were responsible for the increased muscle mass in these myostatin-null mice. Intriguingly, inactivating mutations in the myostatin gene have been identified in double-muscle cattle breeds, sheep and dogs [8-11,12•,13]. Recently, increased skeletal muscle mass as a result of myostatin mutation has even been reported in humans [14••]. These findings indicated that myostatin works as a negative regulator of skeletal muscle growth and development. In adult mice, the inhibition of myostatin resulted in an increase in skeletal muscle by hypertrophy [15•,16]. Therefore, myostatin inhibition is a promising therapeutic approach toward restoring muscle mass and strength in muscle-wasting conditions.

The synthesis and processing of myostatin in the cell is prototypic of members of the TGF-β superfamily [2]. Myostatin is first synthesized as a precursor protein consisting of a signal peptide, an N-terminal propeptide domain and a C-terminal domain (Figure 1). Sequential proteolytic cleavages play a role in myostatin activation. The first cleavage removes the signal peptide, then in the second cleavage, a furin-like protease recognizes the RXRR motif and generates the N-terminal myostatin propeptide and the C-terminal myostatin fragment (Figure 1). It is currently believed that the myostatin precursor forms a homodimer through a disulfide bond before cleavage. The C-terminal dimeric 26-kDa protein acts as the biologically active myostatin, which is referred to simply as myostatin [2].

Figure 1. Sequence alignment of myostatin from various organisms.

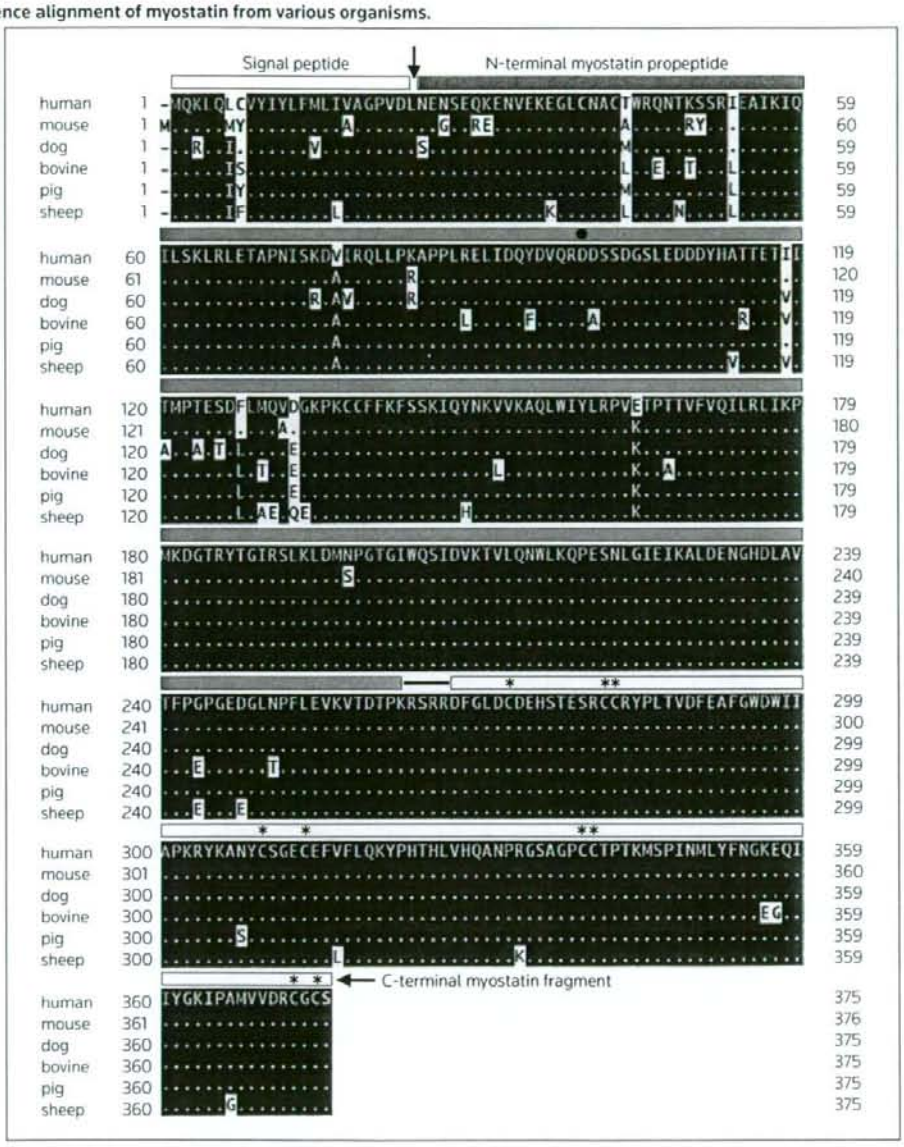

Shaded residues – amino acids matching with the human sequence; Arrow – cleavage site by signal peptidase to remove the signal peptide; Dot – cleavage site by metalloproteinase to activate the myostatin latent complex; Line – RXRR cleavage site by furin-like protease to generate the N-terminal myostatin propeptide and the C-terminal myostatin fragment; White box – signal peptide; Gray box – N-terminal myostatin propeptide; White box with asterisks – C-terminal myostatin fragment; Asterisks – conserved cysteine residues.

Myostatin circulates in serum in a latent form that is complexed with several myostatin-binding proteins (Figure 2) [17•]. Intriguingly, the N-terminal myostatin propeptide remains non-covalently bound to the active myostatin and is a major myostatin-binding protein in serum. The myostatin latent complex can be activated by additional cleavage of the myostatin propeptide by the bone morphogenetic protein-1/tolloid (BMP-1/TLD) family of metalloproteinases [18]. Cleavage occurs between residues Arg^{75} and Asp^{76} of the propeptide (numbered from the N-terminus after signal peptide cleavage) [18]. The mutated form of the propeptide in which Asp^{76} is converted to Ala^{76} (D76A) is resistant to proteolysis and performs as a better myostatin inhibitor than the native myostatin propeptide [19].

Figure 2. Myostatin inhibitors.

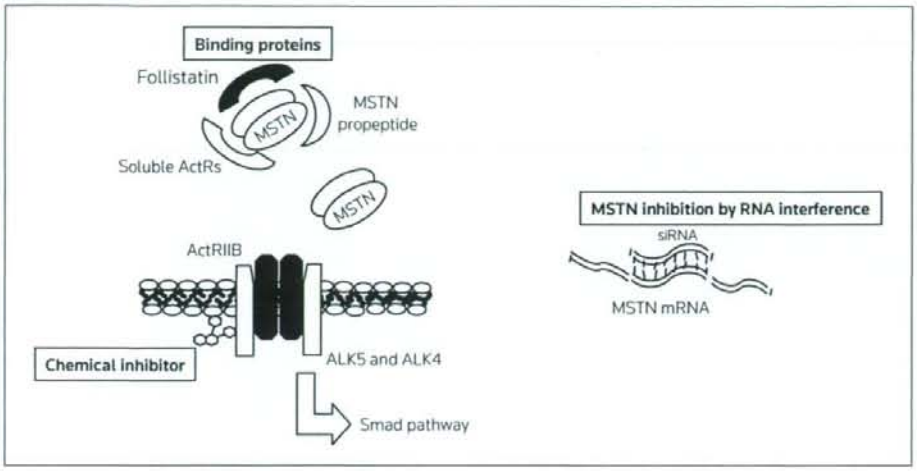

ActR activin receptor, **ALK** activin receptor-like kinase, **MSTN** myostatin, **siRNA** small interfering RNA.

In addition to myostatin propeptide, follistatin-related gene (FLRG) protein and GDF-associated serum protein-1, both of which are follistatin domain-containing proteins, associate with myostatin [17•,20]. Follistatin associates with myostatin both *in vitro* and *in vivo*. Interestingly, these three myostatin-binding proteins are efficient myostatin inhibitors and prevent myostatin from binding to its receptor. In addition, decorin, a small leucine-rich proteoglycan of the extracellular matrix, binds myostatin and regulates its activity in myogenic cells [21]. Recently, it was reported that, unlike in serum, myostatin is present extracellularly as uncleaved pro-myostatin in skeletal muscle, and that an extracellular pro-myostatin constitutes the major pool of latent myostatin in muscle [22]. Thus, the processing of myostatin is regulated in a tissue-specific manner.

Myostatin signaling pathways

Myostatin signals through two types of transmembrane serine/threonine kinase receptors, called type II activin receptors (ActRIIB and ActRIIA) and type I activin receptors (activin receptor-like kinases 5 and 4 [ALK5 and 4]; Figure 2) [5,23•]. The myostatin signaling pathway is similar to that of activin and TGF-β, and is mediated by Smad2 and Smad3 [1,2]. Smad proteins enter cell nuclei upon activation of myostatin and associate with a transcriptional coactivator for gene expression. Increased numbers of satellite cells, which are mononuclear stem cells found between the basal lamina and sarcolemma that are involved in muscle growth, are present in myostatin-deficient mice [24]. One report suggested that myostatin regulates the self-renewal and proliferation of satellite cells by controlling Pax7 expression via the Erk1/2 pathway [24]; however, another recent report demonstrated that myostatin acted *in vivo* to regulate the balance between proliferation and differentiation of embryonic muscle progenitors by promoting their terminal differentiation through the activation of p21 and MyoD [25]. Thus, the effect of myostatin on muscle progenitors is more complex than previously realized and is likely to be context-dependent. Further research is required to elucidate the precise functions of myostatin in muscle.

Myostatin inhibition and therapeutic strategy for muscle-wasting disorders

Myostatin inhibition is effective in increasing skeletal muscle mass and strength, both in the postnatal period and in adults [15•,16]. This suggests that targeting myostatin would be a suitable therapy for muscle-wasting diseases such as muscular dystrophy, cachexia and sarcopenia (Table 1). In particular, a therapy for muscular dystrophy by myostatin blockade will attract clinical attention, as no effective therapy for the disease is available yet. Myostatin inhibition has been reported to be effective in several forms of muscular dystrophies in mouse models, and myostatin antibodies have now been evaluated in human clinical trials [1-4] (see below).

Table 1. Applications of targeting myostatin.

Area of use	Applications
Medical	• Muscle-wasting diseases (eg, muscular dystrophy, cachexia, sarcopenia) • Increasing muscle strength • Diabetes/obesity
Agricultural	• Meat production (bovine, sheep, pig, chicken, fish) • Enhancing racing performance in animals

Cachexia is the severe wasting condition observed in patients with advanced stages of diseases such as cancer and infection. Loss of weight, muscle atrophy and fatigue are evident in cachexic patients. Cachexia is mainly thought to be caused by inadequate food intake, increased metabolic rate and tissue protein breakdown; however, the causes of

cachexia are not fully understood. Systemically administered myostatin induced cachexia with profound muscle and fat loss in mice [26•]. Antagonism of myostatin by follistatin or myostatin propeptide was effective in slowing such myostatin-induced weight loss [26•].

Sarcopenia is derived from the Greek word meaning poverty of flesh, and is the degenerative loss of skeletal muscle mass and strength with aging. The most atrophy is observed in the fast twitch type II myofibers. Multiple factors, including physical inactivity, motor-unit remodeling, decreased hormone levels and decreased protein synthesis, may contribute to sarcopenia. Elevated levels of circulating tumor necrosis factor-α (TNF-α) and adaptations in TNF-α signaling in aged skeletal muscle may be contributing factors in the activation of apoptosis. Short-term blockade of myostatin enhanced muscle regeneration in aged mice after injury and during sarcopenia [27•]. Myostatin antagonism led to satellite cell activation, and resulted in enhanced muscle regeneration in injured aged mice [27•].

Thus, targeting myostatin has significant therapeutic potential in muscle-wasting disorders. In agricultural applications, meat production is the focus of attention (Table 1). It is also of note that racing performance is enhanced in heterozygous myostatin-deficient whippet dogs [12•].

Development of myostatin inhibitors

Myostatin-blocking antibodies

Several myostatin-blocking antibodies have been developed by using phage display technology and protein/antibody engineering [28••,101,102]. Antibody-mediated myostatin blockade in *mdx* mice, a model of Duchenne muscular dystrophy (DMD), was found to ameliorate the pathophysiology and muscle weakness associated with the disease [28••]. This finding indicated that, although normal levels of dystrophin were not regained, myostatin inhibition offers a novel therapy for DMD. The biosafety and effectiveness of the humanized myostatin antibody stamulumab (MYO-029, Wyeth), have been evaluated in clinical studies in the US in patients with muscular dystrophy; however, in February 2008, Wyeth reported it had discontinued development of stamulumab after analysis of clinical data.

Myostatin propeptide

Myostatin propeptide associates with myostatin in serum and works as one of the myostatin inhibitors. Transgenic myostatin propeptide expression prevented muscular atrophy in P104L-mutant caveolin-3 mice [29•]. The myostatin propeptide stabilized by fusion with the immunoglobulin G - fragment crystallizable (IgG-Fc) region was effective in ameliorating the symptoms of *mdx* mice [30]. Myostatin propeptide D76A, in which the Asp^{76} residue was converted to an Ala^{76} residue, was resistant to proteolysis, worked as a better myostatin inhibitor than the native myostatin propeptide [19] and was effective in limb-girdle muscular dystrophy (LGMD) 2A model mice with calpain-3 gene mutations [31].

Soluble myostatin receptors

A soluble form of ActRIIB, also known as ACVR2B, had potent myostatin-inhibitory activity and caused dramatic increases in muscle mass [23•]. Only 2 weeks were required for the soluble form of ACVR2B to increase the muscle mass in mice by up to 60% [23•,103,104]. Because the soluble form of ACVR2B augmented muscle mass even in myostatin-knockout mice, it has been suggested that it also inhibits other ligands, including activins and GDF11, that regulate skeletal muscle growth in addition to inhibiting myostatin [32].

Follistatin and follistatin-related proteins

Follistatin was originally identified as a single-chain polypeptide with weak inhibitory activity toward follicle-stimulating hormone secretion by anterior pituitary cells and was later demonstrated to be an activin-binding protein [33]. Follistatin and FLRG were shown to bind to myostatin and inhibit its activity [34,105] and also induced dramatic increases in muscle mass when overexpressed as transgenes in mice [32]. Follistatin and FLRG are likely to inhibit other regulators of muscle mass with similar activity to myostatin, as overexpression of follistatin or FLRG still caused substantial muscle growth in mice lacking myostatin [32]. Because the inhibition of activin by follistatin was very efficient, follistatin may have effects on skeletal muscles by regulating both myostatin and activin. It was reported that single gene administration of myostatin inhibitors, including follistatin, was enough to enhance skeletal muscle mass for long periods [35].

Recently, the authors developed a myostatin inhibitor derived from follistatin, designated FS I-I, and characterized its effects on muscle mass and strength in *mdx* mice [36••]. Follistatin is composed of an N-terminal domain and three cysteine-rich follistatin domains (FS I, FS II and FS III) [33,37-39]. X-ray crystallographic analyses revealed that the minimal activin-inhibiting fragment of follistatin was comprised of the FS I and FS II domains, and that the individual FS domains may have different activities (Figure 3) [37-39]. A follistatin mutant containing two FS I domains was synthesized, and its binding activities toward myostatin and activin were characterized [36••]. Interestingly, FS I-I retained myostatin binding, but demonstrated significantly weaker activin-binding activity; the dissociation constants of follistatin for activin and myostatin were 1.72 and 12.3 nM, respectively, while, in contrast, the dissociation constants of FS I-I for activin and myostatin were 64.3 μM and 46.8 nM, respectively. Transgenic mice expressing FS I-I under the control of a skeletal muscle-specific promoter showed increased skeletal muscle mass and muscle strength, and hyperplasia and hypertrophy were both observed. FS I-I transgenic mice were crossed with *mdx* mice and characterized. The skeletal muscles in the *mdx*/FS I-I mice were enlarged and showed reduced cell infiltration [36••]. Muscle strength was also recovered in *mdx*/FS I-I mice. These results indicated that myostatin blockade by FS I-I has therapeutic potential for muscular dystrophy [36••]. As myostatin blockade by myostatin propeptide, follistatin and follistatin-derived peptide caused neither an

Figure 3. Crystallography of follistatin bound to activin.

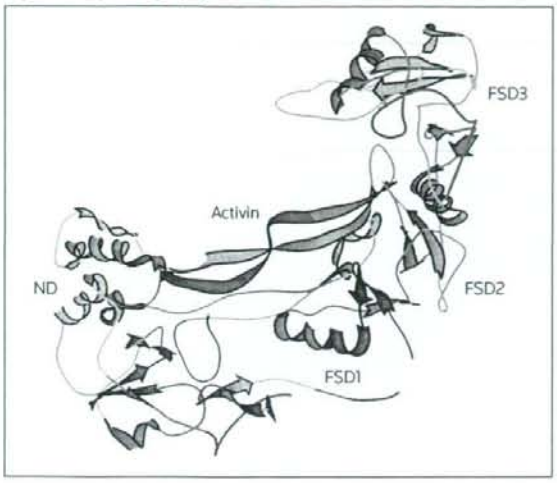

Because the X-ray crystal structure of myostatin is not currently available, structurally related activin is shown. The image is displayed using KiNG software. (*Protein Data Bank DOI: 10.2210.pdb2p6a/pdb*).
FSD follistatin domain, **ND** N-terminal domain.

anti-idiotypic response, nor an antibody-dependent toxic response, they may be superior to myostatin antibody in terms of *in vivo* administration [30]. In addition, follistatin domain-containing proteins associated not only with mature myostatin, but also with myostatin propeptide [20]. Thus, unlike myostatin antibody, follistatin and related proteins may have regulatory functions other than inhibiting mature myostatin activity. It should also be noted that deacetylase inhibitors that are useful for functional and morphological recovery of dystrophic muscle increased the rate of myoblast fusion, leading to enlarged myotubes by the induction of follistatin in satellite cells [40].

Myostatin inhibition by RNAi

RNA interference (RNAi) is a form of post-transcriptional gene silencing (Figure 2). Double-stranded RNA induces degradation of the homologous endogenous transcripts, which results in the reduction or loss of gene activity. A plasmid expressing a short hairpin interfering RNA (shRNA) was designed and electroporated in rat tibialis anterior muscle [41]. RNAi for myostatin was capable of reducing myostatin mRNA and protein, and increasing muscle weight and fiber size *in vivo* [41,42]. Satellite cell number was also increased by more than 2-fold [41]. The RNA oligonucleotide suppressed myostatin expression through upregulation of the MyoD pathway [43]. Importantly, RNA oligonucleotide-dependent myostatin suppression led to the increase in muscle growth both in dystrophic and cachectic mice, as well as in normal mice, indicating a therapeutic potential [42,43]. Thus, myostatin inhibition by RNAi provides an additional opportunity that needs to be investigated further.

Chemical TGF-β inhibitors

ATP-competitive inhibitors of the kinase domain of the TGF-β type I receptor (TβRI, also known as ALK5) have been developed [4,44]. These inhibitors were based on a pyrazole core, and included pyridinylimidazoles and their derivatives (Figure 4). SB-431542 (GlaxoSmithKline plc; Figure 5) was the first selective ALK5 inhibitor to be developed, and it was used as a pharmacological research tool to investigate the role of ALK5 in cellular mechanisms [4]. Treatment with SB-431542 increased lean tissue content and decreased fat content, possibly by inhibiting myostatin *in vivo* [106]. Various small-molecule kinase inhibitors that inhibit the structurally related ALK4, ALK5 and ALK7 at low concentrations have been reported in the patent literature [106,107]. Therefore, chemical TGF-β inhibitors are not specific to myostatin, and inhibit activins and TGF-βs that signal through ALK4, ALK5 and ALK7 [4].

Conclusions

Myostatin is an important regulator that controls skeletal muscle mass. Targeting myostatin has attracted clinical

Figure 4. Crystallography of TGF-β type I receptor kinase with a pyrazole kinase inhibitor.

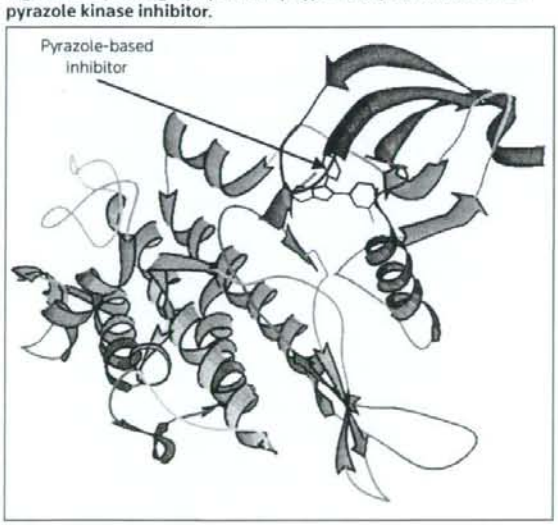

The image is displayed using KiNG software. (*Protein Data Bank DOI: 10.2210.pdb1rw8/pdb*).
TGF-β transforming growth factor-β.

Figure 5. The structure of SB-431542.

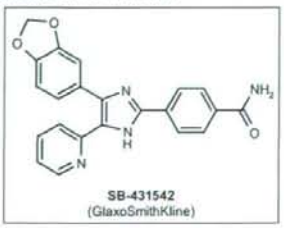

Table 2. Muscular dystrophies and myostatin inhibition.

Disease	Gene locus	Gene products	Myostatin blockage in model animal	Reference
DMD	Xp21	Dystrophin	Effective	[28••,30,36••]
LGMD1C	3p25	Caveolin-3	Effective	[29•]
LGMD2A	15q15	Calpain-3	Effective by gene therapy	[31]
LGMD2F	5q33-34	δ-sarcoglycan	Early therapy is effective	[46]
LGMD2C	13q12	γ-sarcoglycan	Muscle function improved, histopathology not improved	[48]
MDC1A	6q22	Laminin-α2	Not effective	[47]

DMD Duchenne muscular dystrophy, **LGMD** limb-girdle muscular dystrophy, **MDC** muscular dystrophy congenital.

attention for therapy against muscle-wasting disorders such as muscular dystrophy, cachexia and sarcopenia. Myostatin inhibition also has potential in the production of livestock for meat production (Table 1). The processing and production of active myostatin is controlled by multiple processes. Mature myostatin forms a non-covalent, inactive complex with myostatin propeptide, which serves as an inhibitor of myostatin signaling. Physiologically, the BMP-1/TLD family of metalloproteinases cleave myostatin propeptide and this cleavage activates latent myostatin. Myostatin also associates with a number of binding proteins including follistatin and FLRG (Figure 2). Myostatin signals through a combination of activin type II receptors (ActRIIB and ActRIIA) and type I receptors (ALK5 and ALK4; Figure 2). When activated, these receptors phosphorylate Smad2/3, associate with the common Smad4, and then translocate into the nucleus to activate gene transcription [1-6]. In addition to the Smad pathway, multiple non-Smad pathways, including the Erk1/2 mitogen-activated protein kinase pathway and the phosphatidylinositol 3-kinase/Akt pathway, are regulated by myostatin in a context-dependent manner [45].

There are multiple strategies for inhibiting myostatin activity. Myostatin inhibitors, such as monoclonal myostatin antibodies, myostatin propeptide, follistatin, and soluble myostatin receptors, could be lead compounds in drug development for muscle-wasting disorders. Pyrazole-based selective inhibitors of TGF-β type I receptor kinase that are also rational myostatin inhibitors have been developed (Figures 2 and 4). RNAi-based transcriptional degradation of myostatin mRNA is a recently developed strategy for myostatin inhibition (Figure 2).

There are various types of muscular dystrophy, including DMD, LGMDs, and congenital muscular dystrophies (Table 2). Myostatin blockade could be effective in treating these various types of muscular dystrophy and is considered to be most effective when combined with gene correction. In addition to *mdx* mice, two models of LGMDs, caveolin-3 mutation and calpain-3 deficiency, showed pathophysiologies that were ameliorated by myostatin blockade (Table 2) [29•,31]. In the δ-sarcoglycan-deficient LGMD2F model, an age-dependent effect of myostatin inhibition was reported [46]. Myostatin inhibition was beneficial when delivered early, when the disease was relatively mild, whereas it was not effective in the advanced stages of the disease. It was also demonstrated that myostatin blockade was highly variable in its effects on individual muscles [46]. This may reflect the finding that the effect of myostatin was context-dependent in order to regulate the balance between proliferation and differentiation [25]. It should also be noted that myostatin elimination did not combat laminin-α2 deficiency in model mice, but rather increased their postnatal mortality as a result of fat loss [47]. In the case of γ-sarcoglycan-deficient LGMD2C dystrophic mice, myostatin inhibition led to increased fiber size, muscle mass and absolute force; however, no clear improvement in muscle histopathology was evident [48]. One report demonstrated that a lack of myostatin resulted in excessive muscle growth, but impaired force generation [49]. Although the targeting of myostatin had great merit in increasing muscle mass and force, these data disclosed the disease-specific limitations to therapeutic strategies of myostatin blockade in the more severe models of various muscular dystrophies [48].

In summary, recent studies into the development of myostatin inhibitors have been presented and their application and possible limitations as therapies for muscle-wasting disorders have been discussed.

Acknowledgments

This research was supported by grants from the Ministry of Health, Labour and Welfare, and the Ministry of Education, Culture, Sports, Science and Technology of Japan.

References to primary literature

•• of outstanding interest
• of special interest

1. Tsuchida K: **The role of myostatin and bone morphogenetic proteins in muscular disorders.** *Expert Opin Biol Ther* (2006) **6**(2):147-154.

2. Lee SJ: **Regulation of muscle mass by myostatin.** *Annu Rev Cell Dev Biol* (2004) **20**:61-86.

3. Walsh FS, Celeste AJ: **Myostatin: A modulator of skeletal-muscle stem cells.** *Biochem Soc Trans* (2005) **33**(Pt 6):1513-1517.

4. Tsuchida K, Sunada Y, Noji S, Murakami T, Uezumi A, Nakatani M: **Inhibitors of the TGF-β superfamily and their clinical applications.** *Mini Rev Med Chem* (2006) **6**(11):1255-1261.

5. Rebbapragada A, Benchabane H, Wrana JL, Celeste AJ, Attisano L: **Myostatin signals through a transforming growth factor β-like signaling pathway to block adipogenesis.** *Mol Cell Biol* (2003) **23**(20):7230-7242.

6. Tsuchida K, Nakatani M, Uezumi A, Murakami T, Cui X: **Signal transduction pathway through activin receptors as a therapeutic target of musculoskeletal diseases and cancer.** *Endocr J* (2008) **55**(1):11-21.

7. McPherron AC, Lawler AM, Lee SJ: **Regulation of skeletal muscle mass in mice by a new TGF-β superfamily member.** *Nature* (1997) **387**(6628):83-90.
•• *Describes the identification of myostatin, a new member of the TGF-β family that regulates skeletal muscle mass.*

8. Grobet L, Martin LJ, Poncelet D, Pirottin D, Brouwers B, Riquet J, Schoeberlein A, Dunner S, Ménissier F, Massabanda J, Fries R *et al*: **A deletion in the bovine myostatin gene causes the double-muscled phenotype in cattle.** *Nat Genet* (1997) **17**(1):71-74.

9. McPherron AC, Lee SJ: **Double muscling in cattle due to mutations in the myostatin gene.** *Proc Natl Acad Sci USA* (1997) **94**(23):12457-12461.

10. Kambadur R, Sharma M, Smith TP, Bass JJ: **Mutations in myostatin (GDF8) in double-muscled Belgian Blue and Piedmontese cattle.** *Genome Res* (1997) **7**(9):910-916.

11. Clop A, Marcq F, Takeda H, Pirottin D, Tordoir X, Bibé B, Bouix J, Caiment F, Elsen JM, Eychenne F, Larzul C *et al*: **A mutation creating a potential illegitimate microRNA target site in the myostatin gene affects muscularity in sheep.** *Nat Genet* (2006) **38**(7):813-818.

12. Mosher DS, Quignon P, Bustamante CD, Sutter NB, Mellersh CS, Parker HG, Ostrander EA: **A mutation in the myostatin gene increases muscle mass and enhances racing performance in heterozygote dogs.** *PLoS Genet* (2007) **3**(5):e79.
• *Reports the identification of the myostatin gene mutation in racing whippet dogs. Whippets that were heterozygous for a two base-pair deletion in the myostatin gene were in the top racing classes.*

13. Shelton GD, Engvall E: **Gross muscle hypertrophy in whippet dogs is caused by a mutation in the myostatin gene.** *Neuromuscul Disord* (2007) **17**(9-10):721-722.

14. Schuelke M, Wagner KR, Stolz LE, Hübner C, Riebel T, Kömen W, Braun T, Tobin JF, Lee SJ: **Myostatin mutation associated with gross muscle hypertrophy in a child.** *N Engl J Med* (2004) **350**(26):2682-2688.
•• *Reports the identification of the myostatin gene mutation in humans. A German boy with a mutation in both copies of the myostatin-producing gene was hypermuscular. Recently, an American boy born in 2005 with myostatin-related muscle hypertrophy was discovered.*

15. Grobet L, Pirottin D, Farnir F, Poncelet D, Royo LJ, Brouwers B, Christians E, Desmecht D, Coignoul F, Kahn R, Georges M: **Modulating skeletal muscle mass by postnatal, muscle-specific inactivation of the myostatin gene.** *Genesis* (2003) **35**(4):227-238.
• *Reports that inhibition of myostatin results in an increase in skeletal muscle even in the postnatal period.*

16. Welle S, Bhatt K, Pinkert CA, Tawil R, Thornton CA: **Muscle growth after postdevelopmental myostatin gene knockout.** *Am J Physiol Endocrinol Metab* (2007) **292**(4):E985-E991.

17. Hill JJ, Davies MV, Pearson AA, Wang JH, Hewick RM, Wolfman NM, Qiu Y: **The myostatin propeptide and the follistatin-related gene are inhibitory binding proteins of myostatin in normal serum.** *J Biol Chem* (2002) **277**(43):40735-40741.
• *Reports that myostatin circulates in serum in a latent form that is complexed with multiple myostatin-binding proteins.*

18. Wolfman NM, McPherron AC, Pappano WN, Davies MV, Song K, Tomkinson KN, Wright JF, Zhao L, Sebald SM, Greenspan DS, Lee SJ: **Activation of latent myostatin by the BMP-1/tolloid family of metalloproteinases.** *Proc Natl Acad Sci USA* (2003) **100**(26):15842-15846.

19. Lee SJ: **Genetic analysis of the role of proteolysis in the activation of latent myostatin.** *PLoS ONE* (2008) **3**(2):e1628.

20. Hill JJ, Qiu Y, Hewick RM, Wolfman NM: **Regulation of myostatin *in vivo* by growth and differentiation factor-associated serum protein-1: A novel protein with protease inhibitor and follistatin domains.** *Mol Endocrinol* (2003) **17**(6):1144-1154.

21. Miura T, Kishioka Y, Wakamatsu J, Hattori A, Hennebry A, Berry CJ, Sharma M, Kambadur R, Nishimura T: **Decorin binds myostatin and modulates its activity to muscle cells.** *Biochem Biophys Res Commun* (2006) **340**(2):675-680.

22. Anderson SB, Goldberg AL, Whitman M: **Identification of a novel pool of extracellular pro-myostatin in skeletal muscle.** *J Biol Chem* (2008) **283**(11):7027-7035.

23. Lee SJ, Reed LA, Davies MV, Girgenrath S, Goad ME, Tomkinson KN, Wright JF, Barker C, Ehrmantraut G, Holmstrom J, Trowell B *et al*: **Regulation of muscle growth by multiple ligands signaling through activin type II receptors.** *Proc Natl Acad Sci USA* (2005) **102**(50):18117-18122.
• *Reports that myostatin signals through activin type II receptors and that truncated soluble ActRIIB is an efficient myostatin inhibitor in vivo.*

24. McFarlane C, Hennebry A, Thomas M, Plummer E, Ling N, Sharma M, Kambadur R: **Myostatin signals through Pax7 to regulate satellite cell self-renewal.** *Exp Cell Res* (2008) **314**(2):317-329.

25. Manceau M, Gros J, Savage K, Thomé V, McPherron A, Paterson B, Marcelle C: **Myostatin promotes the terminal differentiation of embryonic muscle progenitors.** *Genes Dev* (2008) **22**(5):668-681.

26. Zimmers TA, Davies MV, Koniaris LG, Haynes P, Esquela AF, Tomkinson KN, McPherron AC, Wolfman NM, Lee SJ: **Induction of cachexia in mice by systemically administered myostatin.** *Science* (2002) **296**(5572):1486-1488.
• *Reports that myostatin induced cachexia and that its antagonism is beneficial to slow cachexia in vivo.*

27. Siriett V, Platt L, Salerno MS, Ling N, Kambadur R, Sharma M: **Prolonged absence of myostatin reduces sarcopenia.** *J Cell Physiol* (2006) **209**(3):866-873.
• *Reports that the antagonism of myostatin reduced sarcopenia by regulating satellite cell activation.*

28. Bogdanovich S, Krag TO, Barton ER, Morris LD, Whittemore LA, Ahima RS, Khurana TS: **Functional improvement of dystrophic muscle by myostatin blockade.** *Nature* (2002) **420**(6914):418-421.
•• *Provides the first report that showed myostatin blockade is effective for functional improvement against muscular dystrophy.*

29. Ohsawa Y, Hagiwara H, Nakatani M, Yasue A, Moriyama K, Murakami T, Tsuchida K, Noji S, Sunada Y: **Muscular atrophy of caveolin-3-deficient mice is rescued by myostatin inhibition.** *J Clin Invest* (2006) **116**(11):2924-2934.
• *Reports that myostatin inhibition by myostatin propeptide rescued muscle atrophy of caveolin-3-deficient limb-girdle muscular dystrophy 1C.*

30. Bogdanovich S, Perkins KJ, Krag TO, Whittemore LA, Khurana TS: **Myostatin propeptide-mediated amelioration of dystrophic pathophysiology.** *FASEB J* (2005) **19**(6):543-549.

31. Bartoli M, Poupiot J, Vulin A, Fougerousse F, Arandel L, Daniele N, Roudaut C, Noulet F, Garcia L, Danos O, Richard I: **AAV-mediated delivery of a mutated myostatin propeptide ameliorates calpain 3 but not α-sarcoglycan deficiency.** *Gene Ther* (2007) **14**(9):733-740.

32. Lee SJ: **Quadrupling muscle mass in mice by targeting TGF-β signaling pathways.** *PLoS ONE* (2007) **2**(8):e789.

33. Nakamura T, Takio K, Eto Y, Shibai H, Titani K, Sugino H: **Activin-binding protein from rat ovary is follistatin.** *Science* (1990) **247**(4944):836-838.

34. Takehara-Kasamatsu Y, Tsuchida K, Nakatani M, Murakami T, Kurisaki A, Hashimoto O, Ohuchi H, Kurose H, Mori K, Kagami S, Noji S *et al*: **Characterization of follistatin-related gene as a negative regulatory factor for activin family members during mouse heart development.** *J Med Invest* (2007) **54**(3-4):276-288.

35. Haidet AM, Rizo L, Handy C, Umapathi P, Eagle A, Shilling C, Boue D, Martin PT, Sahenk Z, Mendell JR, Kaspar BK: **Long-term enhancement of skeletal muscle mass and strength by single gene administration of myostatin inhibitors.** *Proc Natl Acad Sci USA* (2008) **105**(11):4318-4322.

36. Nakatani M, Takehara Y, Sugino H, Matsumoto M, Hashimoto O, Hasegawa Y, Murakami T, Uezumi A, Takeda S, Noji S, Sunada Y *et al*: **Transgenic expression of a myostatin inhibitor derived from follistatin increases skeletal muscle mass and ameliorates dystrophic pathology in *mdx* mice.** *FASEB J* (2008) **22**(2):477-487.
•• *Reports the identification of a myostatin inhibitor derived from follistatin. The molecule inhibited myostatin without affecting the activity of activin.*

37. Thompson TB, Lerch TF, Cook RW, Woodruff TK, Jardetzky TS: **The structure of the follistatin:activin complex reveals antagonism of both type I and type II receptor binding.** *Dev Cell* (2005) **9**(4):535-543.

38. Harrington AE, Morris-Triggs SA, Ruotolo BT, Robinson CV, Ohnuma S, Hyvönen M: **Structural basis for the inhibition of activin signalling by follistatin.** *EMBO J* (2006) **25**(5):1035-1045.

39. Lerch TF, Shimasaki S, Woodruff TK, Jardetzky TS: **Structural and biophysical coupling of heparin and activin binding to follistatin isoform functions.** *J Biol Chem* (2007) **282**(21):15930-15939.

40. Minetti GC, Colussi C, Adami R, Serra C, Mozzetta C, Parente V, Fortuni S, Straino S, Sampaolesi M, Di Padova M, Illi B *et al*: **Functional and morphological recovery of dystrophic muscles in mice treated with deacetylase inhibitors.** *Nat Med* (2006) **12**(10):1147-1150.

41. Magee TR, Artaza JN, Ferrini MG, Vernet D, Zuniga FI, Cantini L, Reisz-Porszasz S, Rajfer J, Gonzalez-Cadavid NF: **Myostatin short interfering hairpin RNA gene transfer increases skeletal muscle mass.** *J Gene Med* (2006) **8**(9):1171-1181.

42. Kinouchi N, Ohsawa Y, Ishimaru N, Ohuchi H, Sunada Y, Hayashi Y, Tanimoto Y, Moriyama K, Noji S: **Atelocollagen-mediated local and systemic applications of myostatin-targeting siRNA increase skeletal muscle mass.** *Gene Ther* (2008): epublished ahead of print. DOI:10.1038/gt.2008.24.

43. Liu CM, Yang Z, Liu CW, Wang R, Tien P, Dale R, Sun LQ: **Myostatin antisense RNA-mediated muscle growth in normal and cancer cachexia mice.** *Gene Ther* (2008) **15**(3):155-160.

44. Laping HJ, Grygielko E, Mathur A, Butter S, Bomberger J, Tweed C, Martin W, Fornwald J, Lehr R, Harling J, Gaster L *et al*: **Inhibition of transforming growth factor(TGF)-β1-induced extracellular matrix with a novel inhibitor of the TGF-β type I receptor kinase activity: SB-431542.** *Mol Pharmacol* (2002) **62**(1):58-64.

45. McFarlane C, Plummer E, Thomas M, Hennebry A, Ashby M, Ling N, Smith H, Sharma M, Kambadur R: **Myostatin induces cachexia by activating the ubiquitin proteolytic system through an NF-κB-independent, FoxO1-dependent mechanism.** *J Cell Physiol* (2006) **209**(2):501-514.

46. Parsons SA, Millay DP, Sargent DP, McNally EM, Molkentin JD: **Age-dependent effect of myostatin blockade on disease severity in a murine model of limb-girdle muscular dystrophy.** *Am J Pathol* (2006) **168**(6):1975-1985.

47. Li ZF, Shelton GD, Engvall E: **Elimination of myostatin does not combat muscular dystrophy in dy mice but increases postnatal lethality.** *Am J Pathol* (2005) **166**(2):491-497.

48. Bogdanovich S, McNally EM, Khurana TS: **Myostatin blockade improves function but not histopathology in a murine model of limb-girdle muscular dystrophy 2C.** *Muscle Nerve* (2008) **37**(3):308-316.

49. Amthor H, Macharia R, Navarrete R, Schuelke M, Brown SC, Otto A, Voit T, Muntoni F, Vrbóva G, Partridge T, Zammit P *et al*: **Lack of myostatin results in excessive muscle growth but impaired force generation.** *Proc Natl Acad Sci USA* (2007) **104**(6):1835-1840.

References to patent literature

101. Wyeth/University of Pennsylvania (Walsh FS, Zaleska MM, Howland DS, Holzbaur-Howland E, Tchistiakova L, Karim R, Kelley P, Tan X-Y, Kwak SP, Wallace K, Weber N *et al*): **Antagonist antibodies against GDF-8 and uses in treatment of ALS and other GDF-8-associated disorders.** WO-07024535 (2007).

102. Eli Lilly & Co (Han B, Korytko A, Mitchell PJ, Smith RC, O'Bryan L, Wang R): **Anti-myostatin antibodies.** WO-07044411 (2007).

103. The Johns Hopkins University School of Medicine (Lee S-J, McPherron AC): **Growth differentiation factor receptors, agonists and antagonists thereof, and methods of using same.** WO-02010214 (2002).

104. Wyeth (Wolfman NM, Bouxsein ML): **ActRIIB fusion polypeptides and uses therefor.** WO-04039948 (2004).

105. Wyeth BioPharma (Wood CR, Fitz LJ): **Use of follistatin to modulate GDF-8 and BMP-11.** WO-09945949 (1999).

106. Schering-Plough Ltd (Sawutz DG): **Use of ALK5 inhibitors to modulate or inhibit myostatin activity leading to increased lean tissue accretion in animals.** WO-06025988 (2006).

107. Smithkline Beecham Corp (Dodic N, Donche F, Gellibert FJ): **4-(Heterocyclyl-fused phenyl)-3-(phenyl or pyrid-2-yl) pyrazoles as inhibitors of the ALK-5 receptor.** WO-04111036 (2004).

THE JOURNAL OF GENE MEDICINE
J Gene Med 2008; **10**: 702–713.
Published online in Wiley InterScience (www.interscience.wiley.com) **DOI:** 10.1002/jgm.1190

RESEARCH ARTICLE

Downstream utrophin enhancer is required for expression of utrophin in skeletal muscle

Jun Tanihata[1,2]
Naoki Suzuki[1,3]
Yuko Miyagoe-Suzuki[1]
Kazuhiko Imaizumi[2]
Shin'ichi Takeda[1]*

[1]*Department of Molecular Therapy, National Institute of Neuroscience, National Center of Neurology and Psychiatry, Ogawa-higashi, Kodaira, Tokyo, Japan*

[2]*Laboratory of Physiological Sciences, Faculty of Human Sciences, Waseda University, Mikajima, Tokorozawa, Japan*

[3]*Department of Neurology, Tohoku University School of Medicine, Seiryo-machi, Sendai, Japan*

*Correspondence to:
Shin'ichi Takeda, Department of Molecular Therapy, National Institute of Neuroscience, National Center of Neurology and Psychiatry, 4-1-1 Ogawa-higashi, Kodaira, Tokyo 187-8502, Japan.
E-mail: takeda@ncnp.go.jp

Received: 17 October 2007
Accepted: 30 January 2008

Abstract

Background Duchenne muscular dystrophy is caused by the absence of the muscle cytoskeletal protein dystrophin. Utrophin is an autosomal homologue of dystrophin, and overexpression of utrophin is expected to compensate for the dystrophin deficit. We previously reported that the 5.4-kb 5′-flanking region of the utrophin gene containing the A-utrophin core promoter did not drive transgene expression in heart and skeletal muscle. To clarify the regulatory mechanism of utrophin expression, we generated a nuclear localization signal-tagged LacZ transgenic (Tg) mouse, in which the LacZ gene was driven by the 129-bp downstream utrophin enhancer (DUE) and the 5.4-kb 5′-flanking region of the utrophin promoter.

Methods Two Tg lines were established. The levels of transgene mRNA expression in several tissues were examined by reverse transcriptase-polymerase chain reaction (RT-PCR) and quantitative RT-PCR. Cryosections of several tissues were stained with haematoxylin and eosin and X-gal.

Results The transgene expression patterns were consistent with endogenous utrophin in several tissues including heart and skeletal muscle. Transgene expression was also up-regulated more in regenerating muscle than in nonregenerating muscle. Moreover, utrophin expression was augmented in the skeletal muscle of DUE Tg/dystrophin-deficient *mdx* mice through cross-breeding experiments. We finally established cultures of primary myogenic cells from this Tg mouse and found that utrophin up-regulation during muscle differentiation depends on the DUE motif.

Conclusions Our results showed that DUE is indispensable for utrophin expression in skeletal muscle and heart, and primary myogenic cells from this Tg mice provide a high through-put screening system for drugs that up-regulate utrophin expression. Copyright © 2008 John Wiley & Sons, Ltd.

Keywords downstream utrophin enhancer; Duchenne muscular dystrophy; dystrophin; transcriptional regulation; transgenic mice; utrophin

Introduction

Duchenne muscular dystrophy (DMD) is an X-linked progressive disorder caused by a defect in the DMD gene, which encodes dystrophin [1]. Dystrophin is a 427-kDa cytoskeletal protein that is normally located on the subsarcolemma and fixed by interaction with dystrophin-associated proteins (DAPs), some of which span the membrane [2–5]. This protein complex links the cytoskeleton of myofibers to the extracellular matrix to

maintain the integrity of the sarcolemma. The lack of dystrophin in DMD causes a secondary loss of DAPs in the sarcolemma and leads to massive muscle necrosis, resulting in cardiomyopathy and early death. Unfortunately, there is no treatment available to stop the progression of this devastating neuromuscular disorder other than corticosteroids. Of the various therapeutic strategies for DMD being developed, up-regulation of utrophin has received considerable attention over recent years.

Utrophin is a 395-kDa cytoskeletal protein with a high degree identity with dystrophin at the amino acid level [6,7] and is an autosomal homologue of dystrophin. It is ubiquitously expressed in most tissues. In embryonic and neonatal skeletal muscles, it is expressed both synaptically and extra-synaptically. In adult skeletal muscle, it is found mostly at the postsynaptic membrane of the neuromuscular junction (NMJ) and the myotendinous junction [8,9].

Mdx mice completely lack the expression of dystrophin, but the signs and symptoms of DMD are not progressive until later in the course of the disease. This mild phenotype can be at least partly explained by up-regulation of utrophin at the sarcolemma [10,11]. Additional studies have shown that utrophin is present in greater amounts in small caliber muscle fibers of *mdx* mice [12,13] and small or regenerating muscle fibers of DMD patients [14,15]. By contrast, utrophin null-*mdx* (dko) mice have a severe myopathic phenotype that is lethal within 20 weeks of birth.

Previous transgenic (Tg) experiments showed that over-expression of utrophin at the sarcolemma compensates for the lack of dystrophin and ameliorates dystrophic phenotypes in dystrophin-deficient *mdx* mice, where components of DAPs had been restored [16–18]. Similarly, adenovirally transduced utrophin ameliorates dystrophic changes in *mdx* mice [19]. We previously reported that the immune response to adenovirally transferred β-galactosidase (β-gal) expression evoked up-regulation of endogenous utrophin, resulting in partial improvement of *mdx* phenotypes [20]. These data suggest that systemic up-regulation of utrophin in DMD patients may lead to an effective treatment for this devastating disorder. However, the regulatory mechanism of utrophin expression is not yet fully understood.

Transcriptional regulation of the utrophin gene is more complicated than previously pictured. Two full-length utrophin mRNAs, A and B, which encode different N-termini, are driven by two distinct promoters [21,22]. Both A- and B-utrophin mRNAs are expressed in a tissue-specific manner, and an immunohistochemical study showed that A-utrophin is expressed in the NMJ, choroid plexus, pia mater, and renal glomerulus and tubule [11]. On the other hand, B-utrophin is expressed in vascular endothelial cells [11]. Several short C-terminal utrophin isoforms have been also reported, as found in dystrophin [23]. To elucidate the transcriptional regulation of the utrophin gene, a more powerful tool is engineering an *in vivo* mouse model carrying a reporter gene. We previously generated a transgenic mouse (Gnls) in which the LacZ gene was driven by the 5385-bp 5′-flanking region containing the A-utrophin promoter [24]. Expression of β-gal protein and mRNA derived from the transgene coincided well with the endogenous expression of utrophin in liver, testis, colon, submandibular gland, and small intestine, but β-gal expression was extremely low in skeletal and cardiac muscle. These results suggested that muscle repressor elements may be present in the 5385-bp region or that another regulatory element outside the region might be required for the expression in striated muscle. Comparable results were found by Weir *et al.* [25] by using a transgene covering 3.8 kb of the mouse promoter region, which included the 1.3-kb reporter sequence characterized by Dennis *et al.* [21].

Recently, the downstream utrophin enhancer (DUE) region was identified and located approximately 9 kb downstream of the second intron. The upstream utrophin promoter is under the control of DUE [10,26]. Therefore, in the present study, we generated transgenic mice (DUE Tg) in which DUE was added upstream of the 5385-bp 5′-flanking region and analysed the expression pattern of the transgene in several tissues. We found that the LacZ genes were expressed in skeletal and cardiac muscles. These data are very relevant to finding a way to up-regulate utrophin expression, and DUE mice as well as the primary cells derived from the mice are available for that purpose.

Materials and methods

Construction of transgene and generation of transgenic mice

To further investigate the utrophin A promoter activity in our previous report, genomic fragments containing the 5′ end of the mouse A-utrophin gene were cloned from a 129Sv mouse genomic library (Stratagene, Inc., La Jolla, CA, USA). One clone contained the 5385-bp 5′-flanking region of the A-utrophin gene, the complete exon 1A, and the first 59 bp of the exon 2 untranslated region (UTR). The genomic fragment was fused in-frame to an nls (from SV40T antigen)-tagged LacZ gene [27] (pCMVb; Clontech, San Jose, CA, USA), followed by a rabbit β-globin polyA signal in Bluescript II (Stratagene) [24]. Furthermore, we inserted the 129-bp utrophin enhancer region that is found in utrophin gene intron 2 [26] upstream of this fragment (Figure 1A). The DNA fragment containing the transgene expression cassette was purified from agarose gel and injected into fertilized C57BL/6J eggs by YS Institute (Utsunomiya, Tochigi, Japan) (Figure 1B). We obtained two transgenic F0 (downstream utrophin enhancer/A promoter-nls LacZ transgenic mice), and two transgenic lines were established by mating the founders with C57BL/6J mice (B6) (Figure 1C). To obtain transgenic *mdx* (Tg/*mdx*) male mice, we mated Tg male mice with *mdx* female mice (Figure 1D).

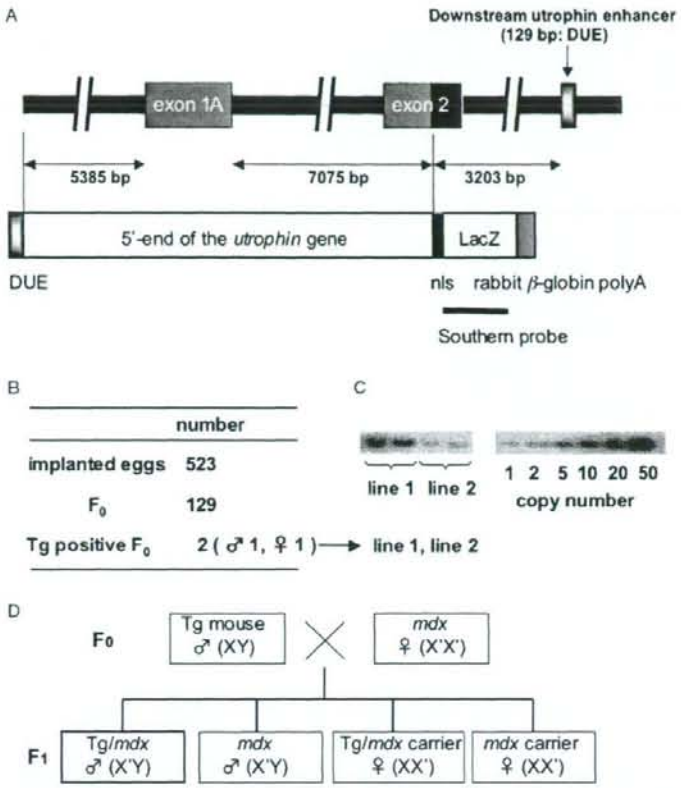

Figure 1. Generation of downstream utrophin enhancer/A-utrophin promoter-nls LacZ Tg mice. (A) Diagram of the transgene used in this study. The genomic fragment (12.9 kb), which contained the 129-bp DUE, 5385-bp 5'-flanking region of the A-utrophin gene, exon 1A, intron 1, and the first 59 bp of exon 2 UTR, was fused in-frame to the nls-tagged LacZ gene. The black bar indicates the Southern probe used to determine genotypes. (B) Summary of generation of Tg mice. (C) Determination of copy numbers in Tg mice by Southern blotting (left). The vector plasmids containing the transgene served as a standard to estimate the number of copies of the transgene (right). (D) Generation of Tg/mdx mice. The bold box indicates the Tg/mdx male mice used in the present study

Animals

C57BL/6J and *mdx* mice aged 5–12 weeks, Tg mice and their wild littermates aged 3–18 weeks, and Tg/*mdx* mice aged 3–7 weeks were used. All animals were housed in a separate room at a temperature of 20–22 °C and under a 12:12 h light/dark cycle. Animals were sacrificed by cervical dislocation. All protocols were approved by the Institutional Animal Care and Use Committee of the National Institute of Neuroscience and were performed in compliance with the 'Guide for the Care and Use of Animals' of the Division of Laboratory Animal Resources.

Genotyping

Tg mice were screened by Southern blotting of genomic DNA from their tails. Genomic DNA was isolated using a lysis buffer [50 mM Tris-HCl, pH 8.0, 0.1 M NaCl, 20 mM ethylenediaminetetraacetic acid, 1% sodium dodecyl sulfate (SDS)] with proteinase K (0.15 mg/ml) and pronase E (1 mg/ml) digestion. Genomic DNA (10 μg) was digested by *BamH*I, separated on a 0.8% agarose gel, and transferred to Hybond-N+ membranes (Amersham Biosciences, Bucks, UK). A 3072-bp DNA fragment of the LacZ gene was labelled with ^{32}P-dCTP as a Southern probe, and hybridized with membranes at 65 °C overnight. The membranes were then washed extensively [2 × saline sodium phosphate-EDTA (SSPE), 0.1% SDS; 1 × SSPE, 0.1% SDS; 0.1 × SSPE, 0.1% SDS] at 65 °C and analysed by BAS 2500 (Fuji Film, Tokyo, Japan).

Isolation of total RNA from mice and myogenic cells

Three- to 8-week-old Tg mice and their wild-type littermates were sacrificed, and tissues were isolated and rapidly frozen in liquid nitrogen. Total RNA was isolated from frozen tissues and myogenic cells using TRIzol reagent (Invitrogen Life Technologies, Carlsbad, CA, USA) according to the manufacturer's protocol.

DOI: 10.1002/jgm

Reverse transcription-polymerase chain reaction (RT-PCR) and quantitative real-time PCR (q-RT-PCR)

RT was performed with 1.0 μg of total RNA using a QuantiTect Reverse Transcription Kit (Qiagen, Valencia, CA, USA) according to the manufacturer's protocol. PCR was performed using LacZ sense (5′-CGACATTGGCGTAAGTGAAG-3′) and antisense (5′-ATCGCCATTTGACCACTACC-3′) primers for 30 cycles (denaturation at 95 °C for 1 min, annealing at 60 °C for 30 s, and extension at 72 °C for 1 min). As a control for the generation of PCR products due to residual contamination of genomic DNA, an equivalent amount of RNA that had not been treated with RT was also processed in parallel. The RT-PCR products of all samples were compared with the levels of a housekeeping gene, 18 s rRNA, amplified with the following primer pair: sense (5′-TACCCTGGCGGTGGGATTAAC-3′) and anti-sense (5′-CGAGAGAAGACCACGCCAAC-3′) primers. The levels of various cDNAs were determined by q-RT-PCR using SYBR Green from ABI PRISM 7700 (Applied Biosystems, Foster City, CA, USA). Each result shows the average of three or four samples. The LacZ and 18 s rRNA primer sequences are described above. A-utrophin: sense (5′-ATGGCCAAGTATGGGGACCTTG-3′) and anti-sense (5′-GTGGTGAAGTTGAGGACGTTGAC-3′) primers; myogenin: sense (5′-CATGGTGCCCAGTGAATGCAACTC-3′) and anti-sense (5′-TATCCTCCACCGTGATGCTGTCCA-3′) primers; and MEF2C: sense (5′-TGGACAACAAAGCCCTC-AGCAGGT-3′) and anti-sense (5′-AATCCCTGCTTCGTTC-CCTCTGC-3′) primers were designed for q-RT-PCR. 18 s rRNA mRNA was amplified as an internal control.

Histochemical analysis

After Tg and wild-type mice were sacrificed, the cerebrum, cerebellum, submandibular gland, lung, liver, kidney, small intestine, colon, testis, tibialis anterior (TA) and gastrocnemius (GC) muscles, diaphragm, and heart were isolated and frozen in liquid nitrogen-cooled isopentane. Cryosections (7 μm) from several tissues were stained with haematoxylin and eosin (H&E) and with 5-bromo-4-chloro-3-indolyl-β-D-galactopyranoside (X-gal; Wako Chemicals, Osaka, Japan) as described previously [28]

Immunohistochemistry

Serial transverse cryosections (7 μm) from different tissues were placed on slides, then dried and fixed in acetone for 10 min at −20 °C. We carried out immunohistochemical analysis with a rabbit polyclonal antibody against human utrophin (UT-2) that recognizes amino acid positions 1768–2078 [29]. The primary antibodies were detected with Alexa 488-labelled goat anti-rabbit IgG (Molecular Probes, Eugene, OR, USA). The nucleus was stained with TOTO-3 iodide (Molecular Probes). The NMJ was stained with Alexa 594-labelled α-bungarotoxin (α-BTX) (Molecular Probes). Signals were recorded photographically with a laser-scanning confocal imaging system (TCSSP; Leica Microsystems, Wetzlar, Germany).

Cardiotoxin injection

To cause muscle degeneration, we injected 100 μl of cardiotoxin (CTX) of *Naja naja atra* venom (10 μM in saline; Wako Chemicals) into the right TA and GC muscles of 5- to 7-week-old Tg mice using a 29-gauge needle. The concentration of CTX was determined as described previously [30]. CTX-injected Tg mice were sacrificed 1–14 days after injection. The CTX-injected and contralateral non-injected TA and GC muscles were isolated and frozen in liquid nitrogen-cooled isopentane. Cryosections (7 μm) were stained with H&E and X-gal. At the same time, serial cryosections (7 μm) were stained with UT-2 together with Alexa 594-labelled α-BTX. Total RNA was isolated from these frozen tissues.

Cell preparation and culture

Mouse-derived mononucleated cells were prepared from DUE and Gnls Tg mice and C57BL/6J mice as previously described [31]. Primary myoblasts were cultured alone with growth medium (GM): F-10 containing 20% fetal bovine serum, 1% penicillin-streptomycin (Invitrogen), and 2.5 ng/ml basic fibroblast growth factor (Invitrogen) in collagen-coated dishes (Iwaki, Tokyo, Japan) or chamber slides (Nalge Nunc, Rochester, NY, USA) coated with collagen type I (Upstate, Waltham, MA, USA). For differentiation, the medium was changed to a differentiation medium (DM; 5% horse serum in Dulbecco's modified Eagle's medium) and cultured 5 days. GM and DM were replenished every 24 h [32].

Statistical analysis

Statistical differences were determined by Student's unpaired *t*-test. All data are expressed as means ± SE. $p < 0.05$ was considered statistically significant.

Results

Generation of downstream utrophin enhancer/A promoter-nls LacZ transgenic (DUE Tg) mice

Two F0 'founder' mice were identified by Southern blotting analysis using a LacZ cDNA probe, and two transgenic lines were established (Figure 1B). The approximate numbers of transgene copies were

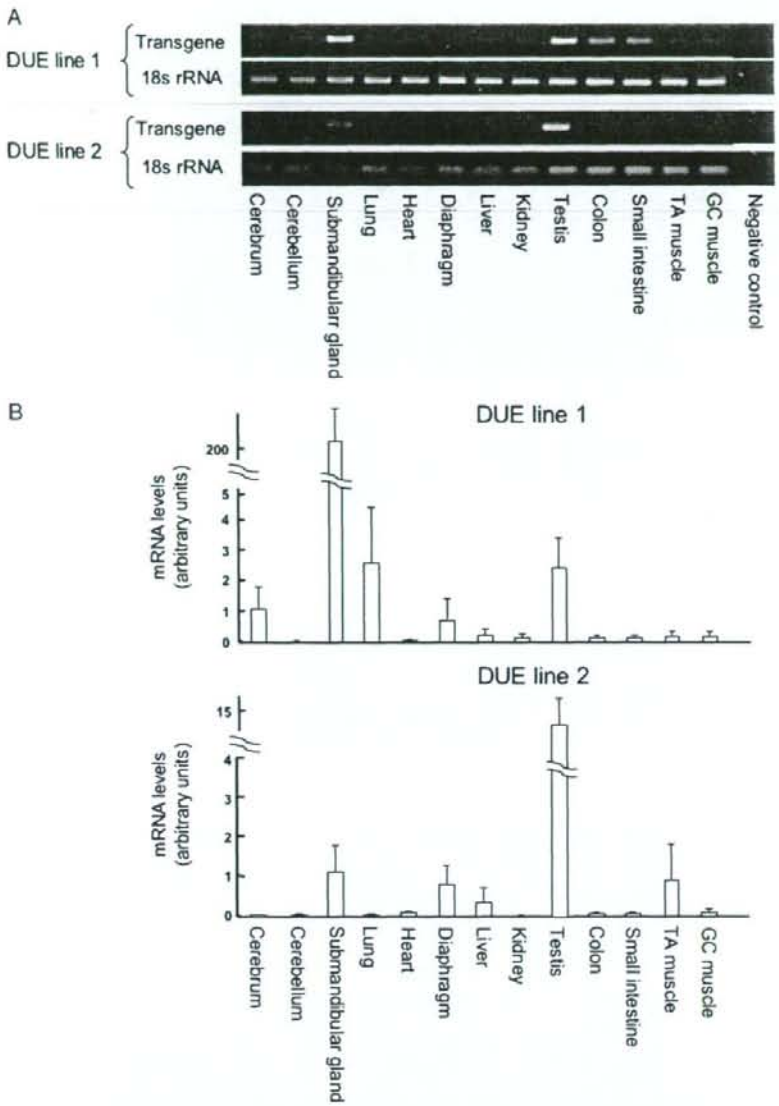

Figure 2. Transgene mRNA expression in several tissues of Tg mice. (A) Representative photomicrographs of EtBr-stained agarose gels depicting cDNA products of the transgene and 18s rRNA from RT-PCR analysis of total RNA from several tissues in Tg mice. (B) Quantification of q-RT-PCR products of the transgene were done by optimization to expression of 18s rRNA in several tissues. The ratio of the transgene to 18s rRNA is shown as the mean ± SEM of four independent experiments performed in triplicate

approximately 15 in line 1 or approximately two in line 2 (Figure 1C).

The levels of transgene expression in several tissues were determined by RT-PCR and q-RT-PCR (Figures 2A and 2B). High levels of transgene mRNA expression were detected in the submandibular gland, testis, lung, colon, and small intestine of DUE line 1 Tg mice and in the submandibular gland and testis of DUE line 2 Tg mice. The signals were weakly detected in other tissues of DUE line 2 Tg mice, probably because there were fewer copies of the transgene.

Comparison of β-gal and endogenous utrophin expression in DUE Tg mice

To compare β-gal expression derived from the transgene with endogenous utrophin expression, cryosections were stained with X-Gal, and then serial cryosections were stained with either H&E or UT-2, a polyclonal antibody against human utrophin [29] (Figure 3). UT-2 recognized only the full-length A- and B-utrophin [29]. We found that β-gal expression coincided well with endogenous utrophin expression in the liver, testis, colon, submandibular gland, small intestine, kidney, and lung (Figure 3A). When

DOI: 10.1002/jgm

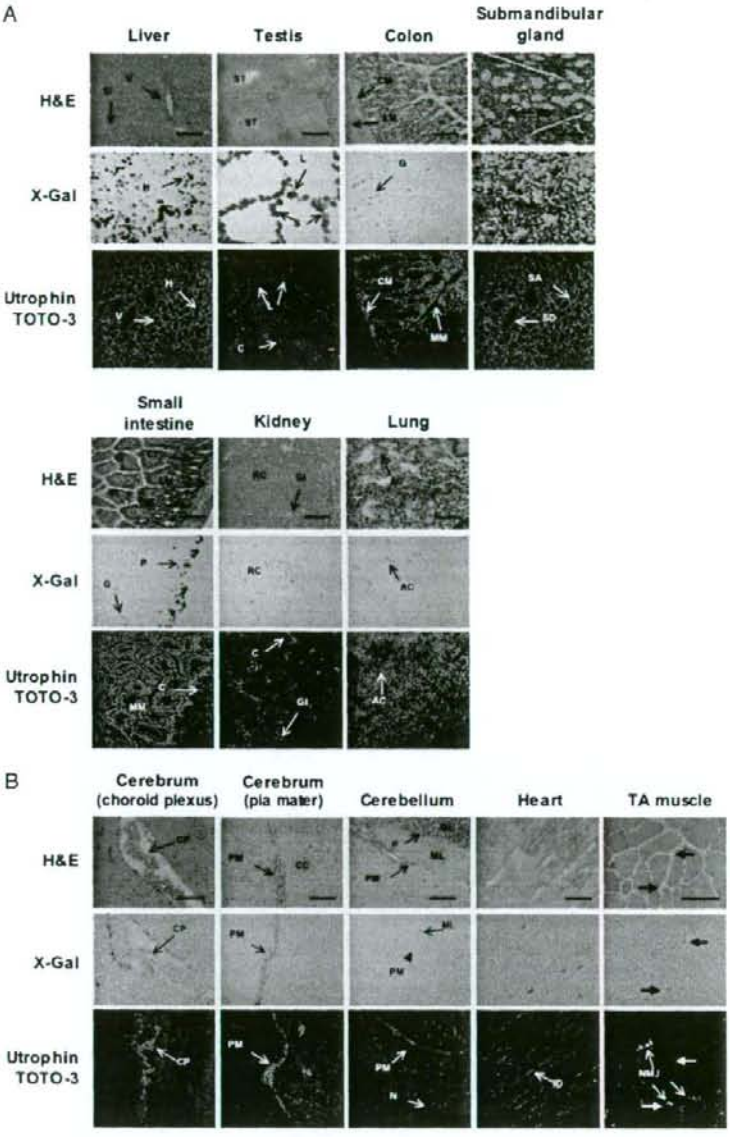

Figure 3. Histological and immunohistochemical analysis of DUE Tg mice. Serial cryosections of tissues [liver, testis, colon, submandibular gland, small intestine, kidney, and lung (A), cerebrum, cerebellum, heart, and TA muscle (B)] from 7-week-old DUE line 1 Tg mice were stained with H&E (top), X-Gal (middle), and a polyclonal antibody against utophin (UT-2; green) (bottom). Nuclei were stained with TOTO-3 (blue). The NMJs were identified with α-BTX (red) in TA muscle. V, terminal hepatic venule; Si, sinusoid; H, hepatocyte; ST, seminiferous tubule; L, Leydig cell; S, Sertoli cell; C, capillary; CM, inner circular muscle layer; G, goblet cell; LM, outer longitudinal muscle layer; MM, muscularis mucosa; SD, striated duct; Sc, serous secretory cell; SA, serous acinus; Vi, villus; Cr, crypt; P, Paneth cell; C, capillary; RC, renal cortex; Gl, glomerulus; AC, alveolar cells; CP, choroid plexus; PM, pia mater; CC, cerebral cortex; N, neuron; ML, molecular layer; GL, granular layer; P, Purkinje cell; ID, intercalated disk; NMJ, neuromuscular junction. Scale bar = 100 μm

compared with β-gal expression in Gnls Tg mice, the expression levels of the transgene in DUE Tg mice were similar in the liver, testis, colon, submandibular gland, and small intestine, but were elevated in the kidney and lung. In addition, when transgene expression was examined at the protein level, the levels were higher in DUE line 1 Tg mice than those in line 2 Tg mice.

In the liver, the nuclei of hepatocytes, but not sinusoid lining cells, were strongly stained with X-gal, whereas endogenous utrophin was detected in the margins of hepatocytes along sinusoids and terminal hepatic venules.

In the testis, β-gal activity was found in Sertoli cells in the basal compartment of the seminiferous tubules, but not in the adluminal compartment, and in Leydig

DOI: 10.1002/jgm

cells in the interstitial supporting tissues between the seminiferous tubules. Consistent with this observation, endogenous utrophin signals were found along the basement membrane of the seminiferous tubules and Leydig cells.

In the colon, β-gal-positive nuclei were found in goblet cells in large intestinal glands. Endogenous utrophin signals were found along the basement membrane of large intestinal glands and the muscularis mucosa.

In the submandibular gland, the nuclei of both serous and mucous secretory cells were clearly stained with X-gal. The striated duct epithelia lacked the β-gal signal. Endogenous utrophin was detected along the basement membrane of serous and mucous acini, but not of striated ducts.

In the small intestine, β-gal-positive nuclei were found in goblet cells and Paneth cells, which lie in epithelia of the bases of villi and crypts. Endogenous utrophin signals were found along the basement membrane of villi and crypts and in the muscularis mucosa.

In the kidney, β-gal-positive nuclei were found in the epithelia of cortical renal tubules, but not in glomeruli. It is not clear whether β-gal positive nuclei were present in proximal convoluted tubules, distal convoluted tubules, collecting tubules, or collecting ducts, although endogenous utrophin was found along the basement membrane of cortical renal tubules, collecting ducts of the renal medulla and Bowman's capsules, and in glomerular capillaries.

In the lung, β-gal-positive nuclei were found in alveoli, but not in terminal bronchiole epithelia. It is not clear whether β-gal-positive nuclei were present in type I or type II pneumocytes. Endogenous utrophin was found in alveolar cells and terminal bronchiole epithelia. In these tissues, endogenous utrophin seemed to localize at the plasma membranes of cells adjacent to the basement membranes.

β-gal expression in cerebrum, cerebellum, heart, and skeletal muscle of DUE Tg mice

In a previous study of Gnls Tg mice, we did not detect any β-gal expression in the cerebrum, cerebellum, heart, and skeletal muscle [24], but we found β-gal expression in these tissues in the DUE line 1 Tg mice (Figure 3B).

In the cerebrum, β-gal positive nuclei were found in ependymal cells of the choroid plexus and in fibroblastic cells of the pia mater along the basal membrane. Consistent with this observation, endogenous utrophin was detected in the choroid plexus and pia mater.

In the cerebellum, β-gal-positive nuclei were found in stellate and basket cells of the molecular layer, but not in fibroblastic cells of the pia mater, although endogenous utrophin is expressed in the pia mater of the cerebellum. Our results indicate that the distal utrophin enhancer cannot activate expression of the transgene in fibroblastic cells of the pia mater in the cerebellum, although it can enhance the expression in fibroblastic cells of the pia mater in the cerebrum.

In the heart, β-gal is expressed in myocardial nuclei located in the vicinity of intercalated disks. Endogenous utrophin expression was found in intercalated disks and T tubules of cardiac muscle.

In skeletal muscle, A-utrophin is expressed in NMJs, peripheral nerves, and larger blood vessels. We detected β-gal expression not only in myonuclei located close to NMJs, but also in myonuclei remote from NMJs in DUE Tg skeletal muscles, although it is not clear whether β-gal-positive nuclei were present in nerves and blood vessels. Expression of the transgene was not detected in the cerebrum, cerebellum, heart, and skeletal muscle in DUE line 2 Tg mice.

β-gal expression was augmented in CTX-injected and dystrophin-deficient DUE Tg mice

We examined expression of the transgene under a condition in which expression of endogenous utrophin is augmented. Recently, Galvagni *et al.* [10] reported that the transcription of A-utrophin was activated in regenerating muscle under DUE control. Therefore, we injected CTX into TA muscles of Tg mice to damage muscle fibers, and analysed β-gal expression during muscle regeneration (Figure 4). The β-gal signals were strongly detected in extrasynaptic regions at 5 or 7 days after CTX injection (Figure 4A). Moreover, transgene mRNA levels were also elevated at 3 or 5 days after CTX injection (Figure 4B). These transgene expressions coincided well with the expression of endogenous utrophin. It is interesting to note that transgene expression was also augmented in CTX-injected DUE line 2 Tg mice, although transgene expression was not detected in non-injected skeletal muscle of these mice (Figure 4C).

Utrophin was also up-regulated in the dystrophic process of *mdx* mouse skeletal muscle. To examine the transgene expression in dystrophin-deficient muscle, we mated DUE line 2 Tg male mice with *mdx* female mice (Figure 1D). Endogenous utrophin was overexpressed along the sarcolemma, and some myonuclei of TA and GC muscles of DUE line 2 Tg/*mdx* male mice were positive for β-gal (Figure 5A). We also found slightly elevated mRNA levels derived from the transgene in TA and GC muscles of DUE line 2 Tg/*mdx* mice by RT-PCR (Figure 5B).

Transgene expression was activated in late stage muscle differentiation *in vitro*

We cultured primary myoblasts from skeletal muscles of DUE Tg and Gnls Tg mice, and some of the cultures were induced to differentiate. Those cells were stained with X-Gal (Figure 6A). Expression of the transgene was detected in primary myoblasts of DUE Tg mice, but

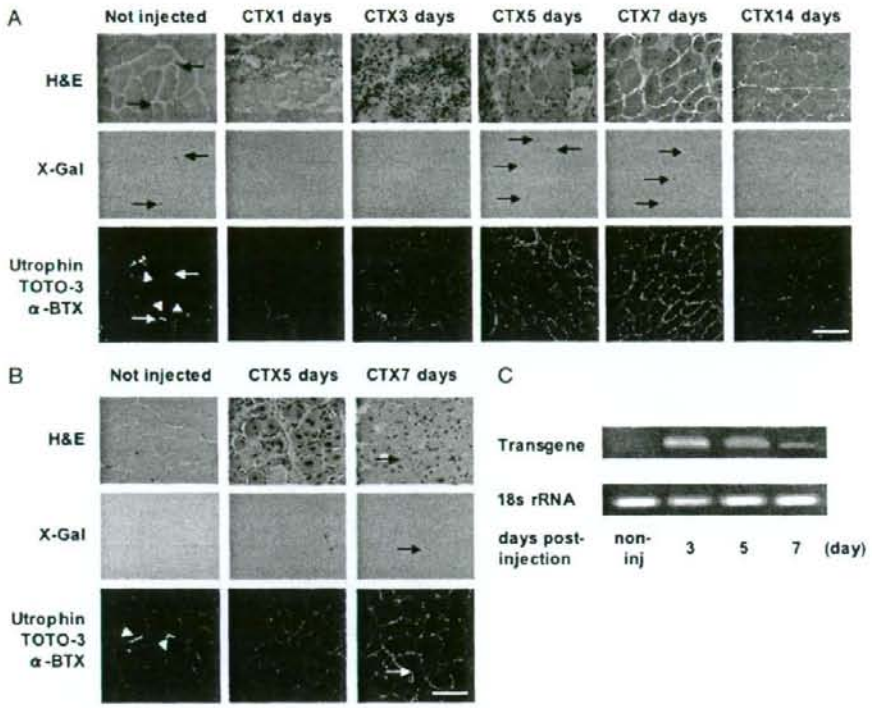

Figure 4. Transgene expression during muscle regeneration in CTX-injected DUE Tg mice. Cryosections of muscles were stained with H&E (top), X-Gal (middle), and a polyclonal antibody against utophin (UT-2; green) (bottom). Nuclei were stained with TOTO-3 (blue). The NMJs were identified with α-BTX (red). (A) TA muscle of DUE line 1 Tg mice at 0, 1, 3, 5, 7, or 14 days after CTX injection. (B) TA muscle of DUE line 2 Tg mice at 0, 5, or 7 days after CTX injection. Arrowhead, NMJ; scale bar = 100 μm. (C) Representative photomicrographs of EtBr-stained agarose gels depicting cDNA products for the transgene and 18s rRNAs from RT-PCR analysis of total RNA from CTX-injected TA muscle of DUE line 1 Tg mice at 0, 3, 5, or 7 days after CTX injection

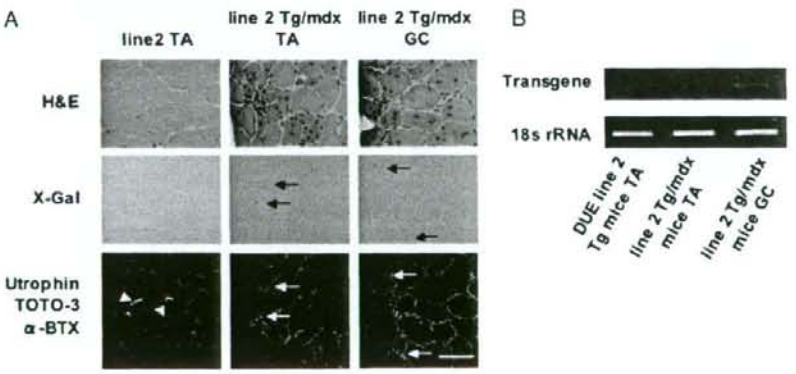

Figure 5. Transgene expression in skeletal muscle of DUE Tg mice cross-bred with dystrophin-deficient mdx mice. (A) Cryosections of muscles were stained with H&E (top), X-Gal (middle), and a polyclonal antibody against utophin (UT-2; green) (bottom). Nuclei were stained with TOTO-3 (blue). The NMJs were identified with α-BTX (red). TA and GC muscles of DUE line 2 Tg/mdx mice. Arrow, β-gal-expressing nuclei; scale bar = 100 μm. (B) Representative photomicrographs of EtBr-stained agarose gels depicting cDNA products for the transgene and 18s rRNAs from RT-PCR analysis of total RNA from TA and GC muscles of DUE line 2 Tg/mdx mice. As a control, the TA muscle of DUE line 2 Tg mice was used

not in those of Gnls Tg mice (Figure 6). In addition, the expression was up-regulated in myotubes in the DUE Tg mice, but not altered in myotubes of the Gnls Tg mice (Figures 6B and 6C). The up-regulation of the transgene was further investigated at the mRNA level, and it was found at a later stage of muscle differentiation. Interestingly, the expression profiles of β-gal and endogenous utrophin were in accordance with that of MEF2C, but not compatible with that of myogenin.

DOI: 10.1002/jgm

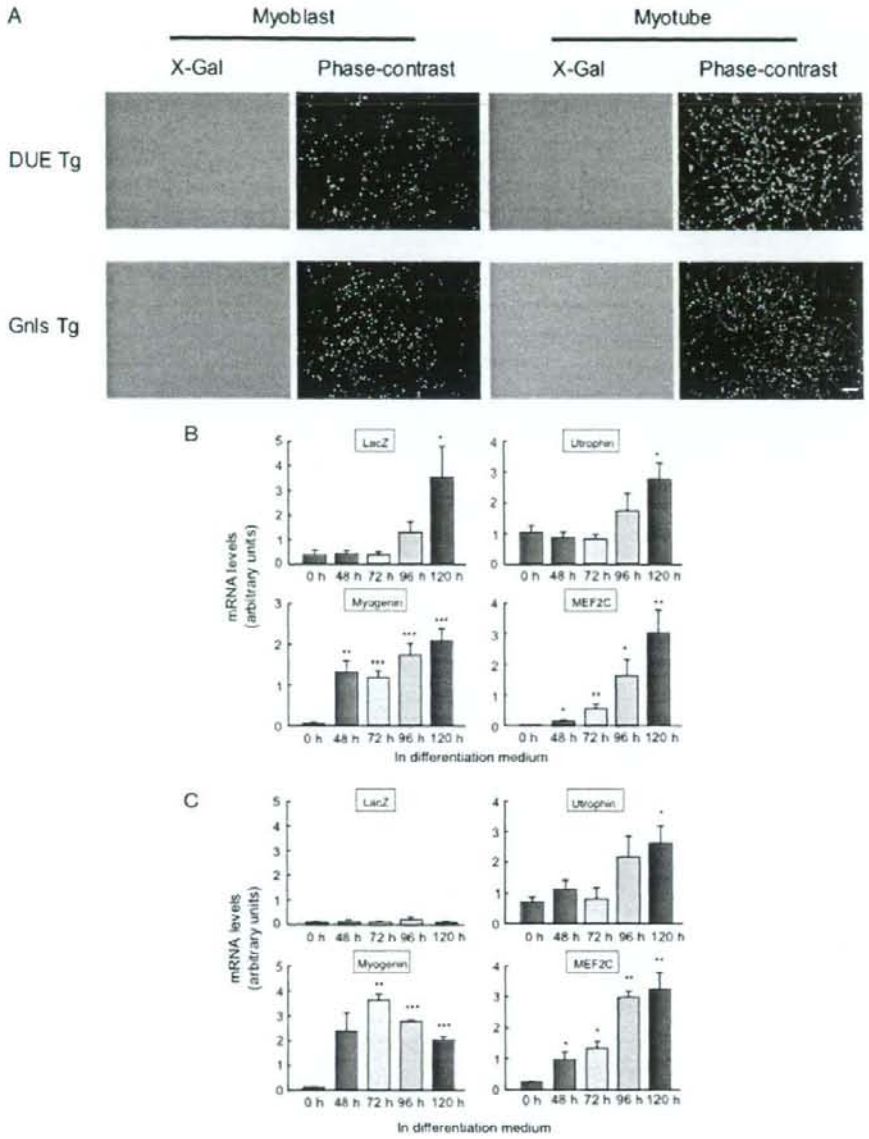

Figure 6. Transgene expression in primary cultured myoblasts and myotubes from DUE Tg mice. (A) Primary cultured myoblasts and myotubes from DUE Tg mice and Gnls Tg mice were stained with X-Gal. Image of myotube after 3 days in differentiation medium. Scale bar = 200 μm. (B, C) Quantification of q-RT-PCR products for transgene, A-utrophin, myogenin, and MEF2C optimized to expression of 18s rRNA in primary myoblasts and myotubes from DUE Tg mice and Gnls Tg mice. The ratios of the transgene, A-utrophin, myogenin, and MEF2C to 18s rRNA are shown as the mean ± SEM of four independent experiments performed in triplicate. *$p < 0.05$, **$p < 0.01$ and ***$p < 0.001$ (versus 0 time)

Discussion

We previously showed that a 5385-bp 5′-flanking region of the utrophin gene containing the A-utrophin core promoter drives high levels of transgene expression in liver, testis, colon, submandibular gland, and small intestine, but not in heart and skeletal muscle [24]. In the present study, we demonstrated that addition of DUE to the 5385-bp 5′-flanking region enabled transgene expression in a pattern that was almost identical to that endogenous utrophin expression (Tables 1 and 2). Moreover, β-gal-expressing nuclei were basically located in the vicinity of the endogenous utrophin expression in heart and skeletal muscle.

In regenerating muscle of DUE Tg mice and skeletal muscle of DUE Tg/*mdx* mice, which lack dystrophin, the transgene expression was considerably

DOI: 10.1002/jgm

Table 1. Cells that express β-gal in Gnls Tg and DUE Tg mice and comparison with endogenous utrophin expression

Tissue	Endogenous utrophin	β-Gal expression		
		Gnls	DUE line 1	DUE line2
Liver	Surface of hepatocyte	Hepatocyte	Hepatocyte	Hepatocyte
Testis	BM of seminiferous tubule	Sertoli cell	Sertoli cell	Sertoli cell
	Leydig cell	Leydig cell	Leydig cell	Leydig cell
Colon	BM of large intestinal gland	Goblet cell	Goblet cell	Goblet cell
	Muscularis mucosa	ND	ND	ND
Submandibular gland	BM of serous & mucous acinus	Serous & mucous secretory cell	Serous & mucous secretory cell	Serous & mucous secretory cell
Small intestine	BM of villus & crypt	Paneth cell, goblet cell	Paneth cell, Goblet cell	Paneth cell, Goblet cell
	Muscularis mucosa	ND	ND	ND
Kidney	BM of cortical renal tubule	Epithelial cell of cortical renal tubule	Epithelial cell of cortical renal tubule	Epithelial cell of cortical renal tubule
	BM of collecting duct in renal medulla			
	Glomerulus	ND	ND	ND
Lung	Alveolus	Alveolar cell	Alveolar cell	Alveolar cell
	Terminal bronchiole epithelium	ND	ND	ND
Cerebrum	Choroid plexus	ND	Ependymal cell of choroid plexus	ND
	Pia mater		Fibroblastic cell of pia mater	
Cerebellum	Pia mater	ND	Stellate cell and basket cell of molecular layer	ND
Heart	Intercalated disk	ND	Peripheral cell of intercalated disk	ND
	T tubule			
Skeletal muscle	Neuromuscular junction	ND	Peripheral cell of neuromuscular junction	ND
	Myotendinous junction			
	Regenerating muscle fiber			

The localization of endogenous utrophin is based on this study and previous studies [11,24]. BM, basement membrane; ND, not detected.

Table 2. Summary of β-gal expression in Gnls Tg mice and DUE Tg mice

	Gnls	DUE line 1	DUE line 2
Liver	++	++	±
Testis	+++	+++	+
Colon	++	++	+
Submandibular gland	+++	+++	+
Small intestine	+	+	±
Kidney	±	+	+
Lung	+	++	±
Cerebrum	−	++	−
Cerebellum	−	++	−
Heart	−	++	−
TA muscle	−	+	−

Tg mice were sacrificed at 4–7 weeks, and β-gal expression was examined in several tissues. No β-gal positive nuclei were found in nontransgenic littermates. β-gal expression levels: −, none; ±, trace; +, weak; ++, moderate; +++, strong.

up-regulated. Another study [10] also reported that utrophin transcription was controlled by DUE activity in regenerating muscle and that its activity was dependent on an AP-1 binding site. Injection of marcain into TA muscles of CD1 mice demonstrated elevation of members of the AP-1 factor, *c-fos, fosB, fra-1, fra-2, c-jun, junB* and *junD* [10]; however, we also found distinct elevation of *c-fos* and *fra-1* mRNA in our regeneration system (unpublished observations).

We cultured primary myogenic cells from DUE Tg mice and found that transgene expression was up-regulated during the differentiation process. Moreover, these transgene expression patterns corresponded to the endogenous utrophin expression profile. This result indicates that the participation of DUE in utrophin expression during muscle regeneration might depend largely on DUE activity in the later stage of muscle differentiation. It is intriguing to note that transgene and endogenous utrophin expression patterns coincided with the expression profile of MEF2C, but not that of myogenin. It has been already reported that MEF2C mediates the promoter activity of c-jun [33]. The MEF2C-c-jun pathway is one of the candidates for regulation of utrophin expression via DUE. Analysis of the transcriptional factors that interact with DUE sequences, particularly the AP-1 site, would be very intriguing and should be clarified by a future study.

In the present study, we also demonstrated that the addition of DUE augmented transgene expression not only in the heart and skeletal muscle, but also in other tissues, such as the cerebral pia mater and choroid plexus and the cerebellar choroid plexus and molecular layer. In addition, transgene expression was elevated in the kidney and lung of DUE Tg mice compared to that of Gnls Tg mice, although it is necessary to consider the difference in transgene copy numbers. These results suggest that DUE activity is not muscle specific, consistent with the data of Galvagni *et al.* [26]. In their study, a construct of DUE added to the utrophin promoter was transiently transfected to various cells and revealed that DUE enhanced utrophin promoter activity not only in C2C12 myoblasts, but also in HeLa cells and RD cells.

However, the addition of DUE cannot fully explain the transcriptional regulation of utrophin. In the cerebrum and cerebellum, endogenous utrophin was expressed in the pia mater and choroid plexus. We found β-gal-positive

DOI: 10.1002/jgm